Journal of Universal Computer Science, vol. 25, no. 6 (2019), 701-717
submitted: 7/1/19, accepted: 20/5/19, appeared: 28/6/19 © *J.UCS*

Quality Assessment of Photographed 3D Printed Flat Surfaces Using Hough Transform and Histogram Equalization

Jarosław Fastowicz
(West Pomeranian University of Technology, Szczecin, Poland
jfastowicz@zut.edu.pl)

Krzysztof Okarma
(West Pomeranian University of Technology, Szczecin, Poland
okarma@zut.edu.pl)

Abstract: Automatic visual quality assessment of objects created using additive manufacturing processes is one of the hot topics in the Industry 4.0 era. As the 3D printing becomes more and more popular, also for everyday home use, a reliable visual quality assessment of printed surfaces attracts a great interest. One of the most obvious reasons is the possibility of saving time and filament in the case of detected low printing quality, as well as correction of some smaller imperfections during the printing process.

A novel method presented in the paper can be successfully applied for the assessment of flat surfaces almost independently on the filament's colour. Is utilizes the assumption about the regularity of the layers visible on the printed high quality surfaces as straight lines, which can be extracted using Hough transform. However, for various colours of filaments some preprocessing operations should be conducted to allow a proper line detection for various samples. In the proposed method the additional brightness compensation has been used together with Contrast Limited Adaptive Histogram Equalization (CLAHE) algorithm. Results obtained for the database of 88 photos of 3D printed samples, together with their scans, are encouraging and allow a reliable quality assessment of 3D printed surfaces for various colours of filaments.

Key Words: additive manufacturing, quality assessment, 3D prints, Hough transform, CLAHE

Category: I.4.6, I.4.10, I.7.5

1 Introduction

The dynamically growing interdisciplinary area of science and industry, related to the applications of computer science, automation, robotics and mechatronic solutions, is one of the key factors of contemporary technology, strongly connected with the idea of "Industry 4.0". Many individual demands, as well as the necessity of relatively fast manufacturing of more or less sophisticated products, are the crucial elements of the modern business and service oriented society.

One of the reasons causing this situation is the rapid development of the additive manufacturing technology and the growing availability and popularity of the 3D printers. This phenomenon concerns mainly the cheapest devices designed for everyday use, based on the Fused Deposition Modelling (FDM) technology, which can be often bought via Internet and built at home.

Since the manufacturing time is often quite long and the overall quality of the 3D printers may be different, the final results of additive manufacturing may be far from expectations. Therefore, one of the recent challenges is related to the visual monitoring of the 3D prints, preferably using the cameras mounted at the 3D printing device, allowing to observe the manufacturing process and take an appropriate action, when necessary. One of the first process monitoring solutions [Cheng and Jafari, 2008] is based on the correlation and dependency between adjacent layers, which have been used for detection of some surface imperfections. A fault detection system proposed in [Szkilnyk et al., 2011] for identification of part jams and feeder jams in automated assembly machines utilizes several webcams and LabVIEW environment for image processing. Nevertheless, as stated by its Authors, it can only detect priorly known faults. Some other fault detection methods proposed for automated assembly machines [Chauhan and Surgenor, 2015, Chauhan and Surgenor, 2017] are based on Gaussian Mixture Models, blob analysis and optical flow, whereas some former solutions utilise the process signatures [Fang et al., 1998, Fang et al., 2003].

Another idea is based on the application of optical coherence tomography (OCT) [Gardner et al., 2018], whereas the application of stereoscopic image analysis compared with the reference 3D model of the manufactured object has been presented in [Holzmond and Li, 2017].

Some other active fields of research concerning the 3D printing issues are related with discovering of microdefects [Straub, 2017b], application of X-ray tomography and ultrasonic imaging [Zeltmann et al., 2016], the use of terahertz non-destructive testing [Busch et al., 2014], as well as thermographic measurements [Lane et al., 2016]. Recently, some cyber-safety and security problems concerning the networked 3D printers have been considered as well [Straub, 2017a, Straub, 2017c, Straub, 2017d].

Apart from the most widely used thermoplastic polymers, known as the polyactic acid (PLA), as well as Acrylonitrile Butadiene Styrene (ABS), some new materials are desired as well, especially considering the toxicity of the ABS fumes. However, development of such new filaments is often application dependent (e.g. materials for some biomedical applications [Ware et al., 2017] have special requirements) and may concern not only thermoplastic materials but also concrete, metal, gum, resin, etc.

2 Machine Vision Solutions for Additive Manufacturing

2.1 Process Monitoring

Regardless of some ideas mentioned above, some more advanced solutions dedicated for 3D printers, utilising the image analysis, have been recently presented. The first approach for early detection of defects [Straub, 2015], allowing to eliminate the necessity of testing the printed objects and potential re-printing, contains a multi-camera system and image processing software. It consists of five cameras and Raspberry Pi units connected via Ethernet cables to the local server. The principle of work of this system is the comparison of in-progress object to the final one using the pixel-by-pixel approach. Therefore, the whole system is very sensitive to small camera motions, as well as changing lighting conditions, and - although working properly - can be considered as an early stage project.

An interesting attempt to the visual monitoring of multi-material 3D printing with the use of the 3D scanning has been presented in the MultiFab platform [Sitthi-Amorn et al., 2015], where the Authors assumed the lack of spatial details and significant textures. Therefore the scanning system based on the Michelson's interferometer and full-field optical coherence tomography (OCT) has been used instead of laser patterns or structured light, typically used in the 3D scanners. Nevertheless, since in low cost FDM printers the individual patterns representing the consecutive layers of the filament can be easily noticed, this approach cannot be directly applied, considering additionally the cost of the OCT based 3D scanner.

Recently, the in situ monitoring solution for the laser powder bed fusion device has been proposed [Scime and Beuth, 2018], which utilises unsupervised machine learning approach for training the classifier. The detection and classification of anomalies occurring during the powder spreading stage can be done using the training database of image patches. Nonetheless, such methods is quite slow as the analysis of a single layer lasts about 4 seconds (according to the Authors' declaration a single 4 GHz i7-4770 processor has been used in experiments). A quite similar approach has also been delivered with the use of trained SVM model [Delli and Chang, 2018] for the single top view camera, although its applicability is limited due to the required interruptions of manufacturing allowing to take photos. The assumption of top view cameras is one of the most troublesome ones in machine vision systems used for the monitoring of the 3D printing. Assuming the applicability of the in situ quality monitoring system for the relatively cheap FDM devices, a much better solution seems to be the use of side view images, where the individual layers can be easily noticed and no breaks of the printing process are necessary to capture the images. Therefore, such assumption has been accepted in our experiments presented later in the article.

2.2 Surface Quality Assessment

Most of the algorithms mentioned above are limited to the observation and automatic analysis of the 3D printing progress allowing to stop the manufacturing process in the case of fault detection. A more desired solution would be the online monitoring of the printed object's quality allowing to correct some detected imperfections or abort the whole printing process after the detection of too low surface quality. Such solutions lead to significant savings of time and filament, especially for relatively big objects, which may be printed even during several hours.

As the topic of automatic surface quality assessment of 3D prints using image analysis is a relatively new area of research, the most similar topics of papers related to computer vision methods, which can be found in literature, are related to various defects detection, e.g. [Laucka and Andriukaitis, 2015]. Nonetheless, the goal of our research concerns the overall quantitative and qualitative evaluation of defects rather then their detection and the first attempts have been made to off-line verification of flat samples' quality.

Therefore, to prevent the influence of unknown lighting conditions, a database of several images of the 3D printed flat samples, acquired using the flatbed 2D scanner with the density of 1200 dpi, has been created. The samples have been obtained using three devices shown in Fig. 1: Prusa i3, RepRap Pro Ormerod 2 and da Vinci 1.0 Pro 3-in-1, using various colours of PLA and ABS filaments. To ensure the presence of some typical distortions in selected samples, the changes of printing parameters have been forced manually, e.g. filament's delivery speed, configuration of stepper motors, temperature, etc. Some of the ABS samples contain individual small cracks as well.

(a) (b) (c)

Figure 1: Three 3D printers used for preparation of samples used in experiments: Prusa i3 (a) RepRap Pro Ormerod 2 (b) and da Vinci 1.0 Pro 3-in-1 (c)

The first part of the dataset containing 16 scanned images of the PLA samples, created for the off-line analysis, has been used in the earliest papers, whereas the remaining 72 images obtained for the ABS filaments have been used for further verification and development of colour independent methods. Technically, the consecutive pairs of images represent both sides of the same 3D prints. The classification should be consistent with subjective evaluation, where each sample has been assessed as low, moderately low, moderately high or high quality. However, among the 16 PLA samples there are only high and low quality ones and therefore the main task remain the classification of surfaces into two main classes representing high and low quality 3D prints.

The second part of the dataset used in our experiments consists of images of the same samples captured by a digital camera in possibly uniform lighting conditions. Nevertheless, the specificity of scans and photos is significantly different and therefore the application of some methods developed for scanned images for the photos is not always straightforward and might be much more troublesome for images acquired by cameras.

Previously developed methods of quality assessment of 3D prints utilise entropy [Fastowicz and Okarma, 2017, Okarma and Fastowicz, 2018] and texture analysis [Fastowicz and Okarma, 2016] with selected Haralick features based on the Gray-Level Co-occurrence Matrix (GLCM) [Okarma and Fastowicz, 2016]. Another investigated approach has been the use of similarity based image quality assessment (IQA) methods [Okarma et al., 2016, Okarma and Fastowicz, 2017], however the direct use of the full-reference (FR) metrics would impose the knowledge of the reference image. Since such reference images of 3D printed surfaces are usually unknown, the use of the FR IQA methods requires their modification allowing the mutual comparison of the image fragments. Another possibility would be the comparison with the model, but for various colours of filaments it would require a colour matching between the models and acquired images.

The application of most previously developed methods for various colours of filaments needs an additional tuning of some parameters, since the results obtained for various materials usually differ significantly. Another disadvantage of some of them can be relatively high computational complexity, e.g. for the methods based on the analysis of the GLCM series [Okarma and Fastowicz, 2016, Fastowicz and Okarma, 2016], limiting their potential future applicability for real-time analysis, especially using low computational power hardware. The best results in terms of colour independent classification have been achieved using the entropy based method [Okarma and Fastowicz, 2018], however this approach has been verified using only the images of several PLA samples with five colours. Hence, the colour independent quality assessment of the 3D printed surfaces, especially assuming a larger dataset of their scans and photos for verification purposes, is still a challenging task, being a motivation of this paper.

3 Proposed Method

Since in low cost FDM printers each layer of the melted filament is placed over the previously hardened material, observing the manufactured object from a side view, the regular linear patterns can be easily noticed, especially for the PLA filaments. Some of the ABS materials allow further removal of such patterns after the additional post-processing. Nevertheless, during the manufacturing or just before the potential smoothing, these patterns can be easily noticed. For the flat surfaces those lines should be straight and oriented horizontally and therefore their detection using the classical Hough transform should be possible. Assuming the necessity of quality assessment of the non-planar surfaces, the application of Circular Hough Transform (CHT) used for finding the fragments of circles instead of straight lines, should be considered.

Nonetheless, both scanned images and photos, especially captured using webcams or low cost cameras with optics introducing some geometrical distortions, may represent the object's surface imperfectly and therefore the detection of long straight lines for planar surfaces may cause some problems. To overcome these issues, as well as the influence of small rotations of the sample and local changes of brightness caused by the lighting conditions, a local detection of lines is proposed, applying Hough transform for the image fragments chosen randomly according to the Monte Carlo method [Okarma and Lech, 2008]. In the presence of some distortions, their importance for the local regions should increase, lowering the number of detected lines.

Obviously, a reasonable number of at least several such blocks should be assumed, as well as their appropriate size, necessary to achieve good detection accuracy for high quality samples. After the experimental verification conducted for the scanned images, reliable and repeatable results have been obtained assuming 40 regions of 150×300 pixels. Since the resolution of full scanned images is 1662×1662 pixels, the additional advantage of the proposed approach is the decrease of the number of analysed pixels by about 35%. An exemplary low quality sample with randomly drawn regions and the detected lines is illustrated in Fig. 2. It is easily predictable that for high quality samples the number and total length of the detected lines would be higher and therefore the first idea of the metric would be the use of the average length of detected lines in all regions.

The simplified flowchart of the proposed method is illustrated in Fig. 3. As can be noticed, its first step is related to conversion of colour images, scanned or captured by a camera, into greyscale. Such images are subjected to further binarization, however, due to some problems with binarization of images obtained for samples made using various colours of filaments, caused mainly by changes of contrast, the additional preprocessing step has been introduced before the thresholding. The best results for the scanned samples have been obtained using the popular ITU Recommendation BT.601-7 (used in MATLAB's

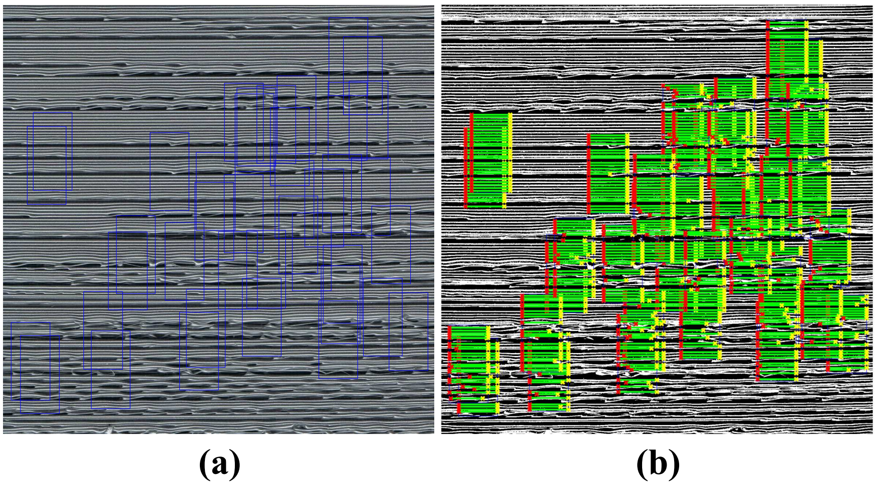

Figure 2: One of the low quality samples with randomly drawn regions (a) and lines detected using Hough transform shown with the result of binarization (b)

rgb2gray function). The additional correction of images is made by the application of the Contrast Limited Adaptive Histogram Equalization (CLAHE) algorithm [Zuiderveld, 1994].

The next step of experiments has been the choice of the appropriate parameters for the CLAHE algorithm to ensure possibly best classification of samples into high and low quality groups. The best results have been achieved applying the exponential histogram distribution with the parameter $\alpha = 0.9$ for 256 bins with the clip limit set to 0.1. Another investigated parameter has been the number of tiles, into which the image should be cut. After the experimental verification the optimal choice for the scans turned out to be the default value for the MATLAB's *adapthisteq* function, namely 8×8 tiles.

The influence of the binarization method on the obtained results has not been so critical, however the use of an inappropriate method may also cause some problems. Although many more or less sophisticated binarization methods have been proposed in recent years, mainly intended for document image binarization [Shrivastava and Srivastava, 2016], our experiments have been concentrated rather on the use of low computationally demanding methods, mainly utilizing the global thresholding. Hence, for the scanned images corrected by the CLAHE algorithm the use of classical Otsu's algorithm [Otsu, 1979] has been enough to achieve reasonably good visibility of lines.

As mentioned earlier, the Hough line detection method has been used for the randomly chosen fragments of the image, however the average length of

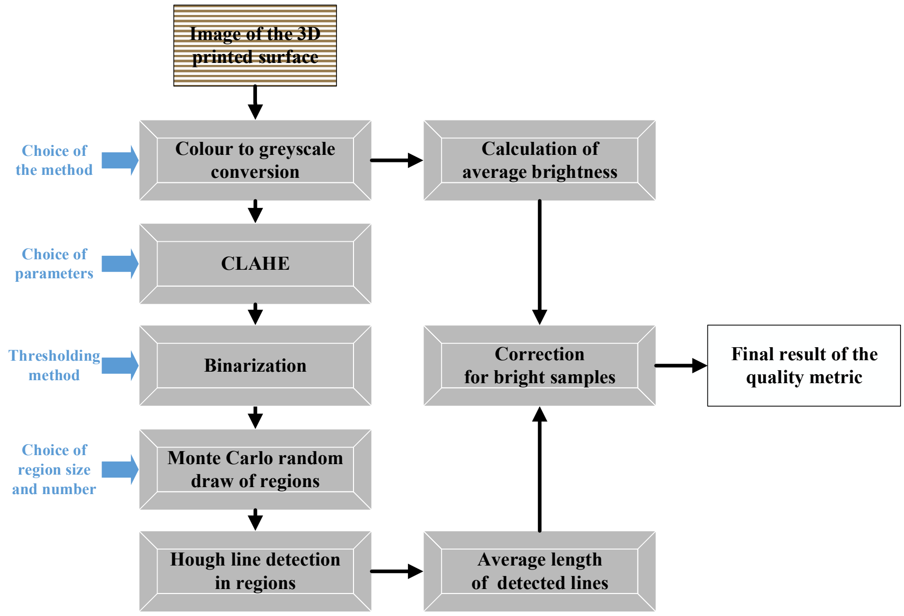

Figure 3: The flowchart of the proposed method with tunable factors influencing the final classification accuracy

the detected lines for the brightest samples has turned out to be smaller. To correct this issue, the additional coefficient dependent on the average brightness of the image has been introduced. For the bright samples - with the normalized luminance $Y > 0.8$ - its value is calculated as $0.02 \cdot M \cdot Y$, assuming the normalized luminance Y within the range $\langle 0; 1 \rangle$ and M as the maximum length of the line, dependent on the size of the region (M=150 according to the chosen size of the region in scanned images). It is worth noticing that in such case the final values obtained for high quality bright samples may be higher than the value of M.

For the convenience of interpretation of obtained results, the natural logarithm of the average length of detected lines with additional correction for bright samples may be used, as shown in Fig. 4, with the threshold value between high and low quality samples equal to 5. As it can be noticed for high quality white and yellow samples (no. 1, 2, 47 and 48), due to the use of additional correction coefficient, the obtained values exceed the upper limit of $\ln(M) \approx 5.01$ indeed. The colours in the plot shown in Fig. 4 reflect the colours of individual samples (although for better visibility the points for the images no. 1–4 have been slightly darkened). The empty symbols denote the presence of cracks and the shapes of the symbols represent the subjective quality of the surface - circles for the high

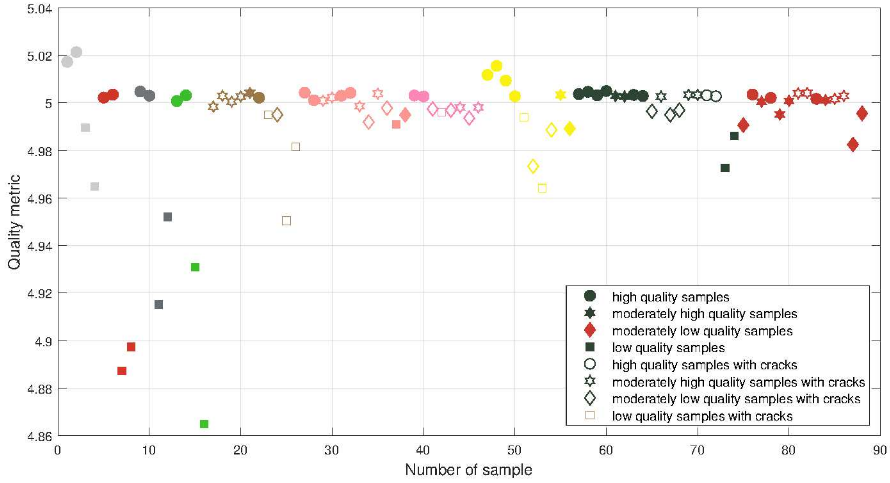

Figure 4: Results obtained for the 88 analysed samples using the proposed approach for scanned images

Number of classified samples				Classification metrics			
TP	FP	FN	TN	Sensitivity	Specificity	Accuracy	F-Measure
50	5	0	33	1	0.868	0.943	0.952

Table 1: Classification metrics obtained for scanned images of the 3D printed samples

quality, stars - moderately high, diamonds - moderately low, and squares for the low quality, as shown in the legend. The same convention has been preserved in the next plots as well. The higher values of the metric should represent high quality samples, whereas lower values (below the threshold) should correspond to the surfaces containing some distortions.

Assuming the properly classified moderately high and high quality samples as true positives (TP) and properly classified distorted surfaces (moderately low and low quality) as true negatives (TN), with false positives (FP) and false negatives (FN) defined consequently for the improperly classified images, some popular classification metrics can be calculated. The four probably most widely used are sensitivity, specificity, accuracy, and F-Measure (known also as F1-score), which are defined as:

$$\text{sensitivity} = \frac{TP}{TP + FN} \,, \tag{1}$$

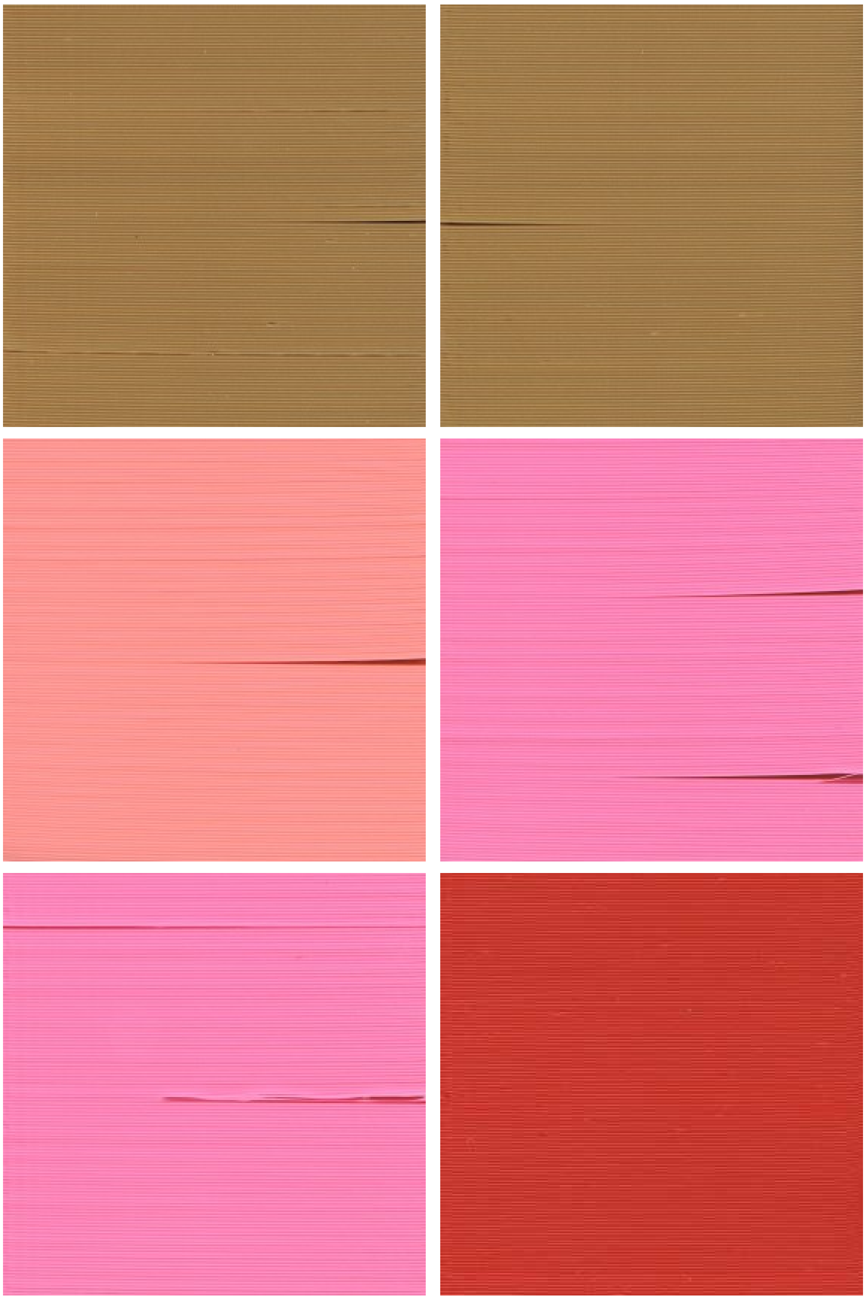

Figure 5: Exemplary scans of the ABS moderate high quality samples no. 17 (upper left) and 18 (upper right), no. 33 (middle left), 44 (middle right), 46 (lower left) and 79 (lower right)

$$\text{specificity} = \frac{TN}{FP + TN} \;, \tag{2}$$

$$\text{accuracy} = \frac{TP + TN}{TP + FP + FN + TN} \;, \tag{3}$$

and

$$\text{FM} = \frac{2 \cdot TP}{2 \cdot TP + FP + FN} \tag{4}$$

respectively. Their values are shown in Table 1.

Analysing the results obtained for scanned images, the appropriate classification of most of the samples can be noticed, especially for high and low quality samples. However, some of the results obtained for individual moderately high quality surfaces require a brief discussion, e.g. the first two brown samples (no. 17 and 18), being in fact the two sides of the same 3D print presented in Fig. 5. They are both subjectively marked as quite similar using the assumed four-level scale, namely moderately high quality with cracks. In fact it can be observed, that the sample no. 17 contains more contaminations, decreasing the overall value of the quality metric to 4.9984 in comparison to 5.0029 achieved for the sample no. 18. Hence, both of them can be considered as border-line examples.

Some other interesting examples are the samples no. 33 (quality 4.9985), 44 (quality 4.9980), 46 (quality 4.9980) and 79 (quality 4.9951), shown in the middle and bottom row of Fig. 5. The quality of the red sample no. 79 seems to be significantly better, even so a proper detection of some of the lines representing consecutive layers might be troublesome due to the presence of many small contaminations. Consequently, the overall quality results is decreased. On the other hand, such a sensitivity of the method to the presence of slight distortions can be an advantage, useful for future combination with some other approaches towards a hybrid metric highly correlated with subjective quality perception and the quantity of visible distortions.

4 Experiments for Photos and Discussion of Results

The direct application of the proposed method for the images of the same 3D printed surfaces, according to expectations, has not led to satisfactory results, and the classification of samples has been much worse as presented in Fig. 6. As can be easily seen, even for the first 16 PLA samples, the samples are mixed and the appropriate threshold could be set only for the silver filament (samples no. 9–12). A proper classification could be independently made for brown ABS material (samples no. 17–26) and red ABS (except the first sample no. 75). Nonetheless, these thresholds would be different for various filaments.

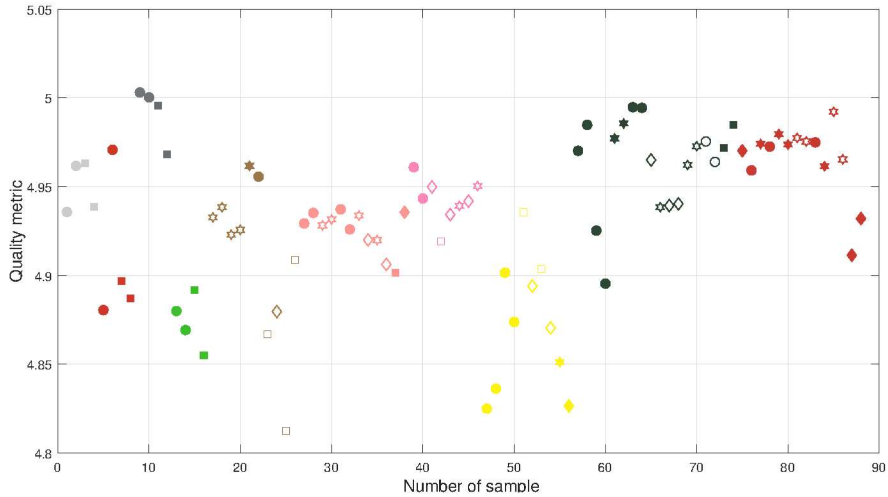

Figure 6: Results obtained for the 88 photos directly applying the approach proposed for scanned images

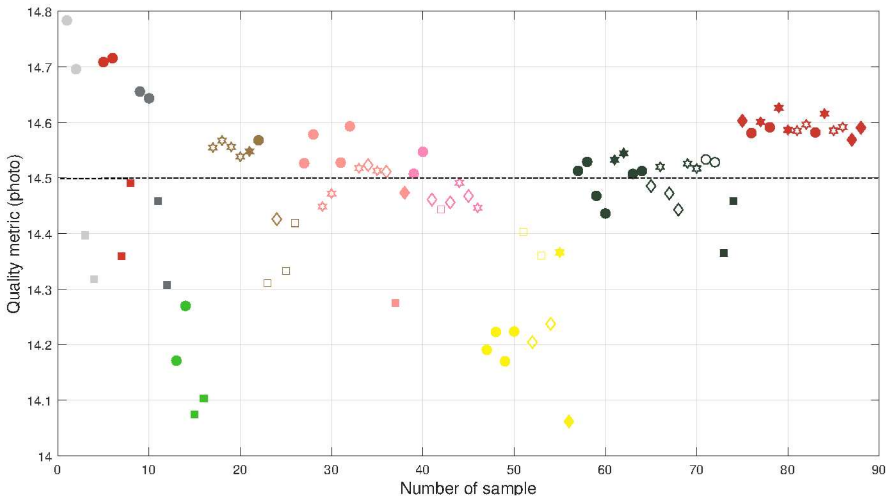

Figure 7: Results obtained for the 88 photos using the proposed modified assessment method

To solve these problems the modified approach has been proposed allowing to preprocess the captured images additionally. Since some of the samples contain some small light reflections, causing some problems in appropriate binarization and further line detection, the oriented horizontal averaging filtering for each line

Number of classified samples				Classification metrics			
TP	FP	FN	TN	Sensitivity	Specificity	Accuracy	F-Measure
42	5	13	28	0.764	0.848	0.795	0.824

Table 2: Classification metrics obtained for photos using the modified approach

has been used with the mask size of 10 pixels, applied before Otsu's thresholding. Before this filter all the images have been subjected to contrast enhancement using MATLAB's *imadjust* function. Both those operations have been applied after the use of CLAHE algorithm.

Furthermore, instead of average length of the detected lines in all the randomly chosen regions, their aggregated length has been used to allow better discrimination between the regions of images containing many regular lines and distorted ones. Finally, instead of the correction for bright samples, the logarithm of the aggregated length of detected lines has been summed with the correction coefficient applied for all images, defined as:

$$\mathrm{C} = \frac{0.02 \cdot Y_{avgC}^{2.15} + 3 \cdot Y_{avgG}}{255}\,, \tag{5}$$

where the values of the coefficients have been tuned experimentally to obtain the maximum possible colour independence of the classification. Two different average image brightness values have been calculated for the original image converted to greyscale (Y_{avgG}) and after the application of CLAHE (Y_{avgC}). Their usage allow to achieve the specificity comparable to scanned images, although the sensitivity of the method has decreased noticeably.

The main reason of the problems is related with too low sharpness of high quality yellow ABS (no. 47–50 and moderately high no. 55) and green PLA samples (no. 13 and 14). Additionally the photos of the green samples contain some small light reflections, which have not been filtered. In both cases the overall length of the detected lines has decreased significantly, lowering the overall values of the calculated quality metrics. This phenomenon is caused by the usage of the automatic depth of field in the camera during the acquisition of images.

Nevertheless, we have decided to leave these images in the experiments to verify and demonstrate the importance of appropriate configuration of cameras according to lighting conditions. Comparing the images obtained for lower quality yellow samples, the results of the proper parameters of the autofocus can be observed and these samples have been classified correctly. Since the proposed method is based on the line detection, their good visibility is a crucial element allowing proper detection of contaminations.

Another issue can be observed for the red ABS samples (no. 75–88), which have been subjectively assessed as slightly worse in comparison to some other

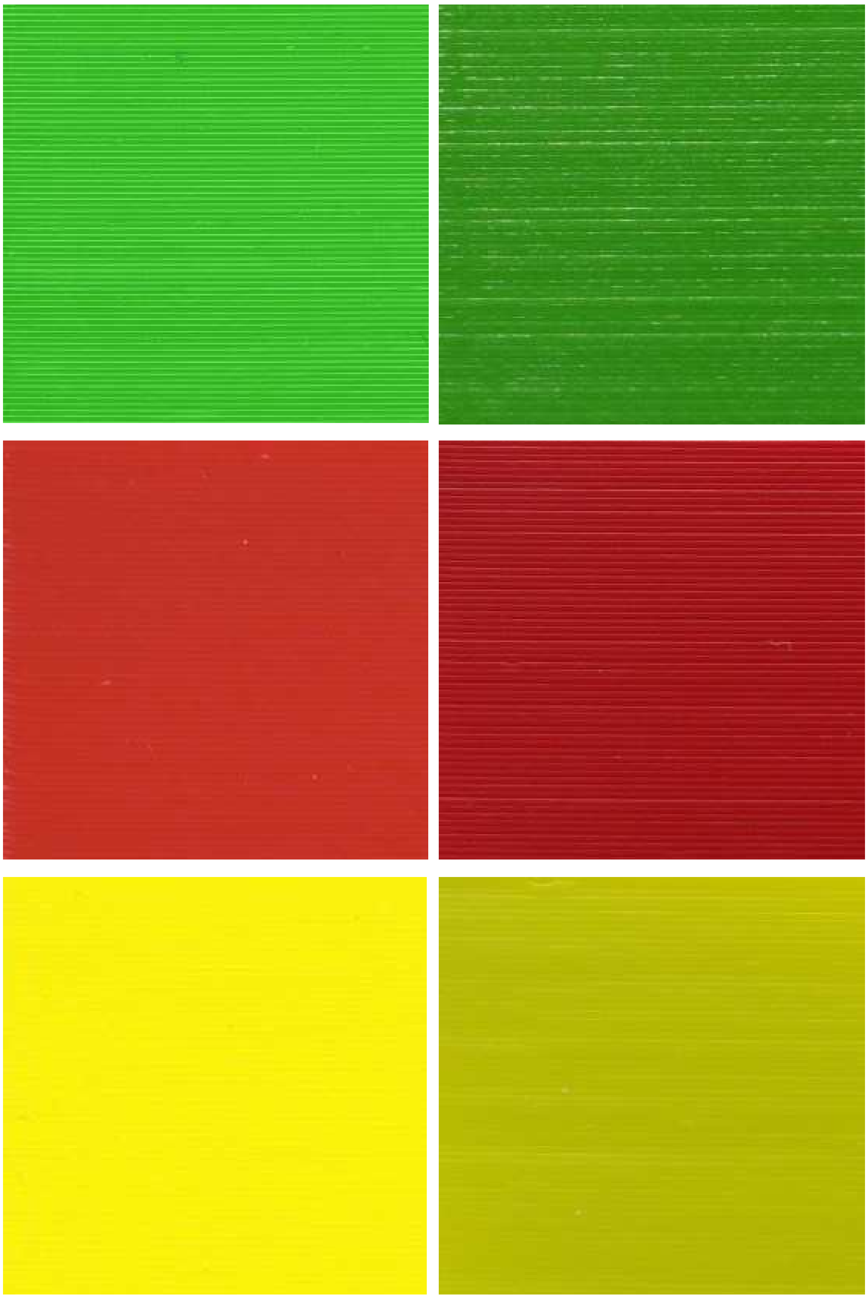

Figure 8: Exemplary scans of the zoomed fragments of some troublesome samples (left) and respective photos (right) illustrating the differences in line visibility

colours. This situation has been caused by the presence of some distortions of the other type than observed in some other samples. The reason of such phenomenon might be related with the specific properties of the filament and potentially absorbed moisture during the additive manufacturing process. The distortions visible on the surfaces of these samples (both for under- and over-extruding) are more smooth and not always influence the continuity of layers, and therefore the length of the detected lines, causing rather the change of thickness of individual layers.

The comparison of some scanned samples and photos (zoomed fragments of the selected samples), illustrating these issues, has been presented in Fig 8.

5 Conclusions and Future Work

The method of automatic quality assessment of the 3D printed surfaces proposed in the paper leads to very promising results, especially for the scanned images. Nevertheless, its modification for the images captured by cameras allow nearly the same classification accuracy, except the images captured with improper configuration of autofocus.

One of the main advantages of the proposed novel methods is their low dependence on the colour of the filament for the popular PLA and ABS materials typically used in low budget devices. In some cases the results may vary, especially for moderate quality samples which are sometimes quite hard also for subjective assessment. Nevertheless, the proposed approach is probably the first original solution, which makes it possible to assess the surface quality of 3D prints automatically and independently on the filament' colour using the images captured by digital cameras.

One of the goals of the planned future work is further tuning of the method, e.g. by a gentle image pre-filtering allowing to remove some very small, almost invisible contaminations which do not influence the properties of the final product, preventing the visibility of cracks and more significant distortions.

Another direction of our future research will be related to some experiments related to the further decrease of the amount of necessary computations, as well as the combination of the presented method with some other recently investigated approaches, e.g. based on texture analysis [Fastowicz and Okarma, 2016] and entropy [Okarma and Fastowicz, 2018].

References

[Busch et al., 2014] Busch, S.F., Weidenbach, M., Fey, M., Schäfer, F., Probst, T., Koch, M.: Optical properties of 3D printable plastics in the THz regime and their application for 3D printed THz optics. Journal of Infrared, Millimeter, and Terahertz Waves 35(12):993-–997, (2014).

[Chauhan and Surgenor, 2015] Chauhan, V., Surgenor, B.: A comparative study of machine vision based methods for fault detection in an automated assembly machine. Procedia Manufacturing, vol. 1, pp. 416-–428, (2015).

[Chauhan and Surgenor, 2017] Chauhan, V., Surgenor, B.: Fault detection and classification in automated assembly machines using machine vision. The International Journal of Advanced Manufacturing Technology 90(9):2491-–2512, (2017).

[Cheng and Jafari, 2008] Cheng, Y., Jafari, M.A.: Vision-based online process control in manufacturing applications. IEEE Transactions on Automation Science and Engineering 5(1):140-–153, (2008).

[Delli and Chang, 2018] Delli, U., Chang, S.: Automated process monitoring in 3D printing using supervised machine learning. Proc. 46th SME North American Manufacturing Research Conference, Procedia Manufacturing 26:865–870, (2018).

[Fang et al., 1998] Fang, T., Jafari, M. A., Bakhadyrov, I., Safari, A., Danforth, S., Langrana, N.: Online defect detection in layered manufacturing using process signature. Proc. IEEE Int. Conf. on Systems, Man and Cybernetics, vol. 5, pp. 4373—4378, (1998).

[Fang et al., 2003] Fang, T., Jafari, M.A., Danforth, S.C., Safari, A.: Signature analysis and defect detection in layered manufacturing of ceramic sensors and actuators. Machine Vision and Applications 15(2):63-–75, (2003).

[Fastowicz and Okarma, 2016] Fastowicz, J., Okarma, K.: Texture based quality assessment of 3D prints for different lighting conditions. Computer Vision and Graphics: International Conference, ICCVG 2016 Proceedings, Lect. Notes in Comp. Sci. 9972, pp. 17–28. Springer International Publishing, (2016).

[Fastowicz and Okarma, 2017] Fastowicz, J., Okarma, K.: Entropy based surface quality assessment of 3D prints. Artificial Intelligence Trends in Intelligent Systems: Proc. 6th Computer Science On-line Conference 2017 (CSOC2017), part 1, AISC, vol. 573, pp. 404-–413. Springer International Publishing, (2017).

[Gardner et al., 2018] Gardner, M.R., Lewis, A., Park, J., McElroy, A.B., Estrada, A.D., Fish, S., Beaman, J.J., Milner, T.E.: In situ process monitoring in selective laser sintering using optical coherence tomography. Optical Engineering, pp. 57:57-–1-–5, (2018).

[Holzmond and Li, 2017] Holzmond, O., Li, X.: In situ real time defect detection of 3D printed parts. Additive Manufacturing 17:135-–142, (2017).

[Lane et al., 2016] Lane, B., Moylan, S., Whitenton, E.P., Ma, L.: Thermographic measurements of the commercial laser powder bed fusion process at NIST. Rapid Prototyping Journal 22(5):778–787, (2016).

[Laucka and Andriukaitis, 2015] Laucka, A., Andriukaitis, D.: Research of the defects in anesthetic masks. Radioengineering 24(4):1033–1043, (2015).

[Makagonov et al., 2017] Makagonov, N.G., Blinova, E.M., Bezukladnikov, I.I.: Development of visual inspection systems for 3D printing. Proc. IEEE Conf. of Russian Young Researchers in Electrical and Electronic Engineering (ElConRus), pp. 1463–1465, (2017).

[Okarma and Fastowicz, 2016] Okarma, K., Fastowicz, J.: No-reference quality assessment of 3D prints based on the GLCM analysis. Proc. 21st Int. Conf. on Methods and Models in Automation and Robotics (MMAR), pp. 788-–793, (2016).

[Okarma and Fastowicz, 2017] Okarma, K., Fastowicz, J.: Quality assessment of 3D prints based on feature similarity metrics. Image Processing and Communications Challenges 8: 8th International Conference, IP&C 2016 Proceedings, AISC, vol. 525, pp. 104—111. Springer International Publishing, (2017).

[Okarma and Fastowicz, 2018] Okarma, K., Fastowicz, J.: Color independent quality assessment of 3D printed surfaces based on image entropy. In: Proc. 10th Int. Conf. on Computer Recognition Systems CORES 2017, AISC, vol. 578, pp. 308—315. Springer International Publishing, (2018).

[Okarma et al., 2016] Okarma, K., Fastowicz, J., Tecław, M.: Application of structural similarity based metrics for quality assessment of 3D prints. Computer Vision and Graphics: International Conference, ICCVG 2016 Proceedings, Lect. Notes in Comp. Sci. 9972, pp. 244-–252. Springer International Publishing, (2016).

[Okarma and Lech, 2008] Okarma, K., Lech, P. (2008). Monte Carlo based algorithm for fast preliminary video analysis. Computational Science – ICCS 2008, Lect. Notes in Comp. Sci. 5101, pp. 790—799. Springer Berlin Heidelberg.

[Otsu, 1979] Otsu, N.: A threshold selection method from gray-level histograms. IEEE Transactions on Systems, Man, and Cybernetics 9(1)62-–66, (1979).

[Scime and Beuth, 2018] Scime, L., Beuth, J.: Anomaly detection and classification in a laser powder bed additive manufacturing process using a trained computer vision algorithm. Additive Manufacturing 19:114—126, (2018).

[Shrivastava and Srivastava, 2016] Shrivastava, A., Srivastava, D.K.: A review on pixel-based binarization of gray images. Proc. Int. Congress on Information and Communication Technology (ICICT), AISC, vol. 439, pp. 357—364. Springer Singapore, (2016).

[Sitthi-Amorn et al., 2015] Sitthi-Amorn, P., Ramos, J.E., Wangy, Y., Kwan, J., Lan, J., Wang, W., Matusik, W.: Multifab: A machine vision assisted platform for multi-material 3D printing. ACM Transactions on Graphics 34(4):129:1–129:11, (2015).

[Straub, 2015] Straub, J: Initial work on the characterization of additive manufacturing (3D printing) using software image analysis. Machines 3(2):55–71, (2015).

[Straub, 2017a] Straub, J.: 3D printing cybersecurity: detecting and preventing attacks that seek to weaken a printed object by changing fill level. Dimensional Optical Metrology and Inspection for Practical Applications VI, Proc. SPIE, vol. 10220, pp. 102200O-–1-–15, (2017).

[Straub, 2017b] Straub, J.: An approach to detecting deliberately introduced defects and micro-defects in 3D printed objects. Pattern Recognition and Tracking XXVII, Proc. SPIE, vol. 10203, pp. 102030L-–1-–14, (2017).

[Straub, 2017c] Straub, J.: Identifying positioning-based attacks against 3D printed objects and the 3D printing process. In: Pattern Recognition and Tracking XXVII, Proc. SPIE, vol. 10203, pp. 1020304—1-–13, (2017).

[Straub, 2017d] Straub, J.: Physical security and cyber security issues and human error prevention for 3D printed objects: detecting the use of an incorrect printing material. Dimensional Optical Metrology and Inspection for Practical Applications VI, Proc. SPIE, vol. 10220, pp. 102200K—1-–16, (2017).

[Szkilnyk et al., 2011] Szkilnyk, G., Hughes, K., Surgenor, B.: Vision based fault detection of automated assembly equipment. Proc. ASME/IEEE Int. Conf. on Mechatronic and Embedded Systems and Applications, Parts A and B, vol. 3, pp. 691-–697, (2011).

[Tourloukis et al., 2015] Tourloukis, G., Stoyanov, S., Tilford, T., Bailey, C.: Data driven approach to quality assessment of 3D printed electronic products. Proc. 38th Int. Spring Seminar on Electronics Technology (ISSE), pp. 300–305, (2015).

[Ware et al., 2017] Ware, H.O.T., Farsheed, A.C., Baker, E., Ameer, G., Sun, Ch.: Fabrication speed optimization for high-resolution 3D-printing of bioresorbable vascular scaffolds. Procedia CIRP 65 (3rd CIRP Conference on BioManufacturing), pp. 131-–138, (2017).

[Zeltmann et al., 2016] Zeltmann, S.E., Gupta, N., Tsoutsos, N.G., Maniatakos, M., Rajendran, J., Karri, R.: Manufacturing and security challenges in 3D printing. JOM 68(7):1872-–1881, (2016).

[Zuiderveld, 1994] Zuiderveld, K.: Contrast limited adaptive histogram equalization. In: Heckbert, P.S. (ed.), Graphics Gems IV, pp. 474—485. Academic Press Professional, Inc., (1994).